Petroleum and Coal

Biodiesel Production from Kitchen Lard via Transesterification by Magnetic Solid Base Catalyst

Sen Qiao[1,2], Rui Wang[1,2]*

[1] *School of Environmental Science and Engineering, Shandong University, No. 27 Shanda South Road, Jinan 250199, China*
[2] *Suzhou Research Institute of Shandong University, No. 388 Ruoshui Road of Industrial Park, Suzhou, 215123, China*

Abstract

A magnetic solid base catalyst (K/CeO_2-Fe_2O_3) was successfully synthesized by sol-gel method which was used to catalyze transesterification of stable kitchen lard and methanol to produce biodiesel. The main components of kitchen lard were analyzed by gas chromatography-mass spectrometer (GC–MS) and the catalysts were characterized by Brunauer-Emmett-Teller (BET), Fourier transform infrared spectroscopy (FT-IR), scanning electron microscope with energy dispersive X-ray (SEM-EDX) and vibrating sample magnetometer (VSM). Results demonstrated that the catalyst had granular nano-structures and superparamagnetism. The optimum conditions for transesterification were found as follows: reaction temperature of 60°C, methanol/oil molar ratio of 6:1 and catalyst amount of 1.5 wt%, corresponding to a maximum biodiesel yield of 92.02% in reaction time of 3 h. Recovery experiment results indicated that the magnetic catalyst maintained high activity after four times' use with a biodiesel yield of more than 84.53%, which would provide the possibility of a potential application to produce biodiesel from waste cooking oil.

Keywords: *biodiesel; magnetic recovery; transesterification; kitchen lard.*

1. Introduction

As a potential substitute of petroleum diesel, biodiesel whose essential component is long chain fatty acid methyl esters (FAME) has stood out in recent decades [1]. Due to its high oxygen content, high flash point, little of sulfur and aromatic content, biodiesel is a kind of renewable, clean, non-toxic and efficient fuel [2]. At present, the main method for industrial production of biodiesel is transesterification of renewable feedstocks like oils and animal fats with methanol or ethanol under the action of the catalyst [3-4]. The transesterification behavior is divided into three synchronous reversible reactions, in which glycerol is collected as byproduct with the production of biodiesel [5].

Generally speaking, the current feedstocks for commercial production of biodiesel are pure refined edible oils such as soybean, canola, sunflower, palm, castor and peanut oil. However, their high price and the threat to worldwide food reserves and safety are major impediments in commercialization of biodiesel [6]. As novel and less costly oily feedstocks, the non-edible oils, microalgae, waste cooking oil, animal fats, and other sources can take place of edible oils for biodiesel production [7-8].

Previously, homogeneous acids and bases including HCl, H_2SO_4, NaOH, and CH_3ONa were used as catalysts for the transesterification reaction, and they have already been conducted on a commercial scale using [9]. Unfortunately, there are many problems for these homogeneous catalysts such as high corrosiveness, difficulty for recovery and large amount of wastewater production [10]. In contrast, heterogeneous catalysts used for biodiesel production by transesterification reactions have been found to be easily separated from the reaction system,

thereby simplifying the production process [11]. Liu *et al.* [12] used CaO as a solid base catalyst for transesterification from soybean oil to biodiesel. Under optimal conditions, the biodiesel yield could exceed 95% at 3 h. Shu *et al.* [13] synthesized a solid acid catalyst from sulfonation of an incompletely carbonized organic compound, and the maximum conversion rate reached 94.8% after 4.5 h.

As a basic catalyst, cerium oxide (CeO_2) is not active in transesterification reactions, but it is a good candidate as carrier for homogeneous acid or base catalysts to improve the catalytic efficiency because of its larger specific surface with plenty of active sites and high catalytic activity [14]. Wong *et al.* [15] synthesized solid base CaO–CeO_2 mixed oxide catalysts via transesterification from palm oil to produce biodiesel. The biodiesel yield could achieve 95% by this catalyst under the optimum reaction conditions. Similarly, Ca-doped Ce-SBA-15 catalyst was successfully synthesized by using direct synthesis of Ce-incorporated SBA-15 followed by impregnation of CaO for biodiesel production [16]. However, the studies on transesterification process using KOH–CeO_2 catalyst are scarce.

In this paper, the fat pork was used to refine lard which was to simulate stable waste cooking oil to be used as the raw material for transesterification. And the magnetic solid base catalyst K/CeO_2-Fe_2O_3 was synthesized by sol-gel method to catalyze this reaction. The transesterification of kitchen lard with methanol to biodiesel using KOH loaded on magnetic ceria as solid base catalyst has been studied by investigating the role of reaction time, catalyst dosage and ethanol-to-oil molar ratio. The main components of kitchen lard were analyzed by gas chromatography-mass spectrometer (GC–MS) and the synthesized solid base catalysts were characterized by Brunauer–Emmet–Teller method (BET), fourier transform infrared (FT-IR) spectra, scanning electron microscope-energy dispersive X-ray (SEM-EDX) and vibrating sample magnetometer (VSM). The characterization results demonstrated that the mesoporous CeO_2 which was magnetized by Fe_2O_3 and loaded by KOH was successfully synthesized. The effect of its separation and reuse was remarkable. The studies showed that the biodiesel yield could reach 92.02% under the optimal preparation and reaction conditions. The catalyst could be recycled and used more than 4 times with high efficiency.

2. Materials and methods

2.1. Materials

Fat pork was obtained from supermarket (Jinan, China). Polyoxyethylene ether (Brij35) was purchased from Macklin (Shanghai, China). Ceric ammonium nitrate ($Ce(NH_4)_2(NO_3)_6$), ethanol, methanol, n-hexane, ammonia solution (25 wt%), potassium hydroxide (KOH), ferrous chloride tetrahydrate ($FeCl_2 \cdot 4H_2O$) and six hydrated ferric chloride ($FeCl_3 \cdot 6H_2O$) were procured from Sinopharm (Shanghai, China). Heptadecanoic acid methyl ester, hexadecanoic acid methyl ester, oleic acid methyl ester, octadecanoic acid methyl ester, 11-octadecenoic acid methyl ester and 9, 12-octadecadienoic acid methyl ester were purchased from J&K (Beijing, China). All the chemicals were analytical regent and used without further purification. Deionized water was used for dissolution and dilution of chemical solutions.

2.2. Preparation of catalyst

The CeO_2 carrier was synthesized by soft template method [17]. Brij35 and $Ce(NH_4)_2(NO_3)_6$ were mixed with a molar proportion of 2:1 and dissolved into 50% ethanol solution. Then, 25 wt% ammonia was added drop-wise into the solution to regulate pH to 10.0. The resultant solution was filtered and washed with ethanol and deionized water twice respectively. Then it was stirred for 3 h and statically aged for 2 d. The collected residue was dried in a vacuum oven at 80°C for about 6 h and then calcined at 350°C in a muffle furnace.

The K/CeO_2-Fe_2O_3 catalyst was obtained by sol-gel method. The obtained CeO_2 carrier was dissolved into deionized water. The solution was stirred for 2 h and treated by sonication for 0.5 h. The $FeCl_3 \cdot 6H_2O$ and $FeCl_2 \cdot 4H_2O$ with a mole ratio of 2:1 were simultaneously added into the above CeO_2 solution with constantly stirring by polytetrafluoroethylene agitator for about 1 h. The ammonia was added into the above solution at room temperature until the pH of the

solution was maintained at about 11.0. After 1 h of strong stirring, the resultant solution was aged for 2 h. Then it was dialyzed over deionized water until the washing solution became neutral. After being freeze-dried and shattered, magnetic carrier CeO_2-Fe_2O_3 was synthesized. The CeO_2-Fe_2O_3 was dipped into aqueous solutions of KOH with loading amount of 40% and subsequently vacuum dried at 120 °C for 12 h. After being crushed into powder with a mortar, the dried material was calcined in a muffle furnace at 300°C for 3 h to obtain the final magnetic solid base catalyst K/CeO_2-Fe_2O_3.

2.3. Transesterification reaction

In this article, kitchen lard was used to simulate stable waste cooking oil. Raw material was refined from the fat pork in a pan. The kitchen lard was filtered to remove the impurities of fat pork after the frying process. Before production of biodiesel, the filtered lard was pre-treated by heating at a 90°C water bath pot for about 2 h. The process of transesterification was carried out in a 250 mL neck flask with a certain proportion of lard, methanol and catalyst. The neck flask was put into a water bath equipped with a stirrer and a water-cooled condenser at certain temperature for transesterification. The solution was stirred for 4 h, and the upper liquid phase was sampled every 0.5 h. After rotary evaporation and centrifugation, the collected samples became biphasic. The purified biodiesel was produced in the upper phase transformed from kitchen lard.

After transesterification process was completed, the magnetic catalyst was separated and recycled from the mixture by a permanent magnet. Then, the recycled catalyst was cleaned by methanol and dried in an oven at 70°C for about 5 h. Finally, it was put into a desiccator for further use.

The products was dissolved into n-hexane and analyzed by a gas chromatograph (GC, SP-6800) equipped with a capillary column (AT-FFAP: 30 m×Φ 0.32 mm×0.33 μm) and a flame ionization detector (FID) detector. The yield of fatty acid methyl ester (FAME) can be calculated by using the following equation:

$$Y_{FAME} = \frac{\sum f_e A_e}{A_i} \times \frac{m_i}{m_e} \times 100\%$$

where, Y_{FAME} is the yield of fatty acid methyl ester, f_e is the correction factor of each fatty acid methyl ester that biodiesel contains, A_e is the peak area of corresponding fatty acid methyl esters, A_i is the peak area of the internal standard, m_i is the mass of internal standard and m_e is the mass of fatty acid methyl esters.

The recovery of the catalyst is described as follows:

$$R_c = \frac{w_1}{w_2} \times 100\%$$

where, R_c is the recovery of catalyst, w_1 is the weight of the recovery catalyst and w_2 is the weight of the added catalyst.

2.4. Biodiesel sample analysis

Gas chromatography-mass spectrometer (GC–MS) method was used to determine the main components of biodiesel. The samples were analyzed by a GCMS-QP2010Plus (Shimadzu, Japan) equipped with a flame ionization detector (FID) and an Rxi-Wax capillary column (30 m×Φ 0.25 mm×0.25 μm). The total flow rate of carrier gas (helium) was maintained at 44.0 mL/min. The final product was injected at 250°C with a split ratio of 1:44. At the same time, the temperature of detector was also 250°C. At first the oven temperature was fixed at 160°C for 1min. Next, the temperature was increased to 200°C at 5°C /min and then kept for 1 min. Last, it was increased to 230°C at 2°C /min and then held it for 5 min.

2.5. Catalyst characterization

The specific surface area was calculated from the adsorption curve by the Brunauer-Emmett-Teller (BET) method using ASAP2020 (Micromeritics, USA). The mesoporous volume and pore size distribution were calculated according to the Barrett-Joyner-Halenda (BJH)

method from the desorption branch of the isotherm. FT-IR spectra of the samples were carried out with ALPHA-T Fourier transform infrared spectrometer (BRUKER Corp, Germany). Scanning electron microscope with energy dispersive X-ray (SEM-EDX) analysis was performed to examine the surface structure and morphology of the catalyst with JSM7610F (Hitachi, Japan). Magnetization curves were measured on a vibrating sample magnetometer (VSM) on a LDJ9500 instrument (USA) with a magnetic field of 10,000 Oe.

3. Results and discussions

3.1. Analysis and characterization

3.1.1. GC-MS of biodiesel

The main components of biodiesel detected by GC-MS are presented in Fig.1. Table.1 shows main components and their content. They were hexadecanoic acid methyl ester, oleic acid methyl ester, octadecanoic acid methyl ester, 11-octadecenoic acid methyl ester, 9, 12-octadecadienoic acid methyl ester respectively and a small amount of other fatty acid methyl esters.
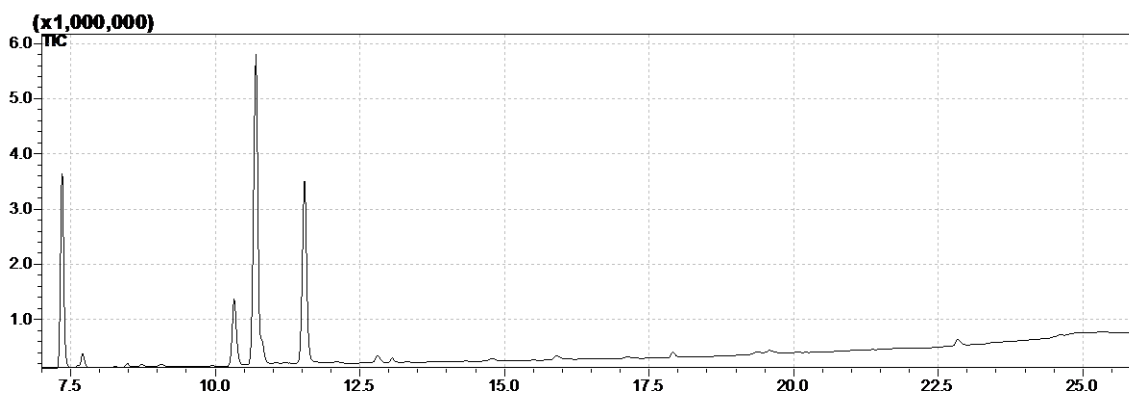
Fig.1 GC-MS spectrum of produced biodiesel

Table.1 GC-MS date of the produced biodiesel

Peak no.	Retention time (min)	Identified methyl esters	Corresponding fatty acids	Composition (%)
1	7.36	Hexadecanoic acid methyl ester	C16:0	19.59%
2	7.77	Oleic acid methyl ester	C18:1	1.53%
3	10.32	Octadecanoic acid methyl ester	C18:0	8.62%
4	10.69	11-Octadecenoic acid methyl ester	C18:1	42.75%
5	11.55	9,12-Octadecadienoic acid methyl ester	C18:2	23.77%
		Other fatty acid methyl esters		3.74%

3.1.2. BET

The specific surface area, pore volume and pore size of CeO_2 before and after calcination are presented in Table 2. This carrier has the specific surface area of 169.98 m^2/g, pore volume of 0.078 cm^3/g and average pore diameter of 3.24 nm.

The N_2 adsorption-desorption isotherms and pore diameter distributions of the CeO_2 carrier are shown in Fig.2. According to the IUPAC classification, the N_2 adsorption-desorption isotherms belong to type IV with an H2 hysteresis loop which is associated with the capillary

condensation of typical mesoporous materials [18]. The main pore diameters are mainly distributed in the range of 0-10 nm. This also proves that the synthesized CeO_2 is mesoporous.
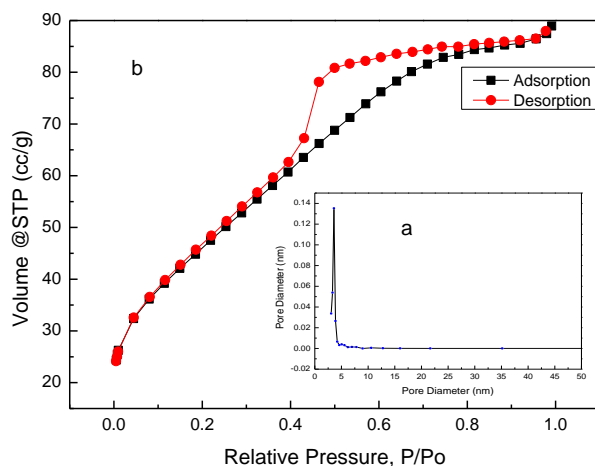
Fig.2. CeO_2 after being calcinated at 350°C (a) pore size distribution curves, (b) nitrogen adsorption-desorption isotherm

Table.2 Physical properties of CeO_2 before and after calcination

Type	Specific surface area (m²/g)	Pore volume (cm³/g)	Most probable pore size (nm)	Average pore width (nm)
Before calcination	163.759	0.068	3.067	3.09612
After calcination	169.98	0.078	3.31	3.24

3.1.3. FT-IR

The functional groups of the materials are elucidated by FT-IR absorption spectra of in Fig.3. All samples show characteristic absorption band at 3447 and 1625 cm^{-1}, which represent the stretching vibration and bending vibration of O-H, respectively. The broad bands at 1120 and 1385 cm^{-1} be attributed to the presence of C-O and C-H. The existence of the peak at 515 cm^{-1} is the telescopic vibration of Ce-O. The characteristic bands of Fe-O-Fe stretching vibration can be found around 600 cm^{-1}, which indicates the catalyst contains magnetic components. The peak at 487 cm^{-1} can be seen as the lattice vibration of the metal oxide KO_x produced from the decomposition of KOH [19].
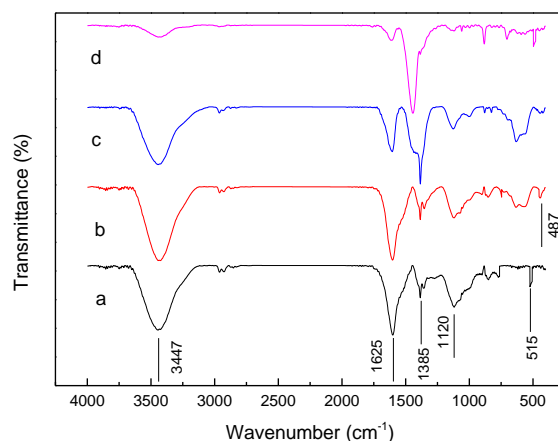
Fig.3. FT-IR absorption spectra of (a) CeO_2, (b) magnetic CeO_2, (c) precursor, (d) magnetic catalyst of K/CeO_2-Fe_2O_3

3.1.4. SEM-EDX

Fig.4a and Fig.4b show the surface micrographs of CeO_2 and K/CeO_2-Fe_2O_3. Fig.4c and Table.3 are the EDX image and analysis of K/CeO_2-Fe_2O_3.

The micrograph of CeO_2 exhibited massive structure and K/CeO_2-Fe_2O_3 displayed cluster shape particles of mutual accumulation evenly. The surface element contents of catalysts are listed in Table.3. O, K, Ce, Fe and some minor components can be seen in the EDX spectra. The contents indicated that the K and Fe were well loaded on the surface of CeO_2.
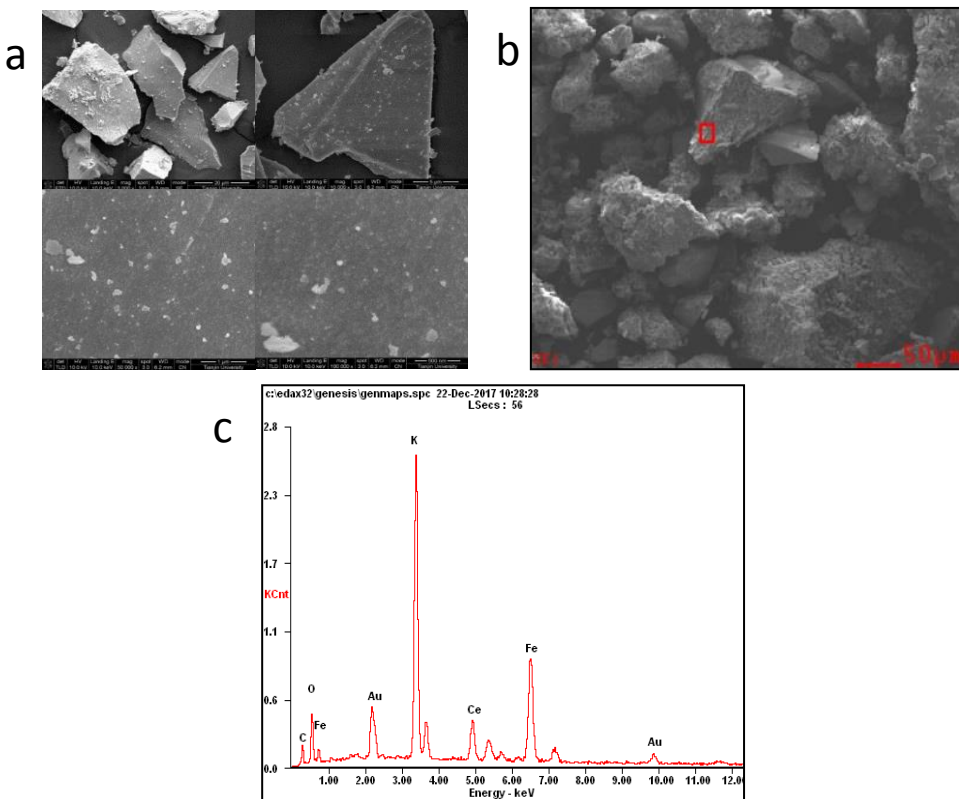
Fig.4 SEM of images of (a) CeO_2, (b) magnetic catalyst of K/CeO_2-Fe_2O_3 and EDX image of (c) magnetic catalyst of K/CeO_2-Fe_2O_3

Table.3 EDX analysis of K/ CeO_2-Fe_2O_3

Element	Wt %	At %
O	10.46	29.06
K	30.63	34.82
Ce	22.50	7.14
Fe	36.41	29.98

3.1.5. VSM

The magnetic properties of K/CeO_2-Fe_2O_3 were measured using VSM and the resulting magnetization curves are presented in Fig.5 which shows the magnetic hysteresis loops for different recovery times. It can be concluded that these catalysts possessed ferromagnetic characteristic and exhibited superparamagnetism, because all curves go through the zero point. As the number of recovery increases, the saturation magnetization becomes weaker, and the saturation magnetization changed from 10.73 emu/g to 7.29 emu/g after four times' recycle, which might be the loss of the magnetic substrates.
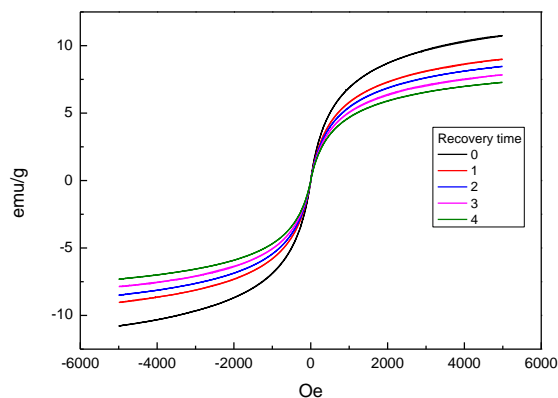
Fig.5 VSM images of different recycle time

3.2. Influence of reaction parameters

3.2.1. Effect of the transesterification conditions

To determine the effect of transesterification conditions, three main factors: reaction temperature, methanol/oil molar ratio and catalyst amount were investigated. Fig.6. exhibits the effect of the transesterification conditions under the optimum preparation conditions of catalyst.

The variations of biodiesel yield after 3h under different reaction temperature are shown in Fig.6a with methanol/oil molar ratio of 6:1 and catalyst amount of 1.5%. It can be seen that with the increment of reaction temperature from 50°C to 60°C, the yield of biodiesel rise from 82.41% to 92.02%. However, as reaction temperature increased continuously, the biodiesel yield decreased significantly because the methanol bubbles out at 64.7°C. Hence, the optimum reaction temperature for the transesterification is 60°C.

Fig.6b shows the variations of biodiesel yield of different methanol/oil molar ratio with catalyst amount of 1.5% under 60°C after reacting for 3h.
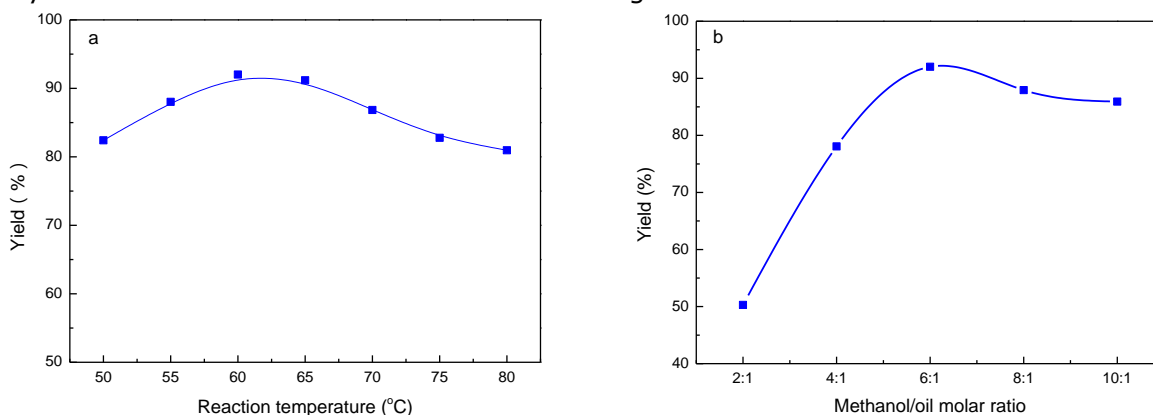
Fig.6. Effect of (a) reaction temperature on yield

Fig.6. Effect of (a) reaction temperature, (b) methanol/oil molar ratio on yield

The biodiesel yield rose from 50.29% to 92.02% with the methanol/oil molar ratio increased from 2:1 to 6:1. However, the yields decreased gradually when the methanol/oil molar ratio rose to 8:1 and 10:1. Because the transesterification reaction is a reversible reaction, excessive methanol/oil molar ratio more than theoretical value of 3:1 is necessary to promote the reaction. The equilibrium of the reaction moves forward with the methanol/oil molar ratio improved to 6:1. Excessive use of methanol will dilute the whole reaction system, causing the deactivation of catalyst and reducing the contact area of oil and catalyst. Besides, too much amount of methanol might make it difficult to separate biodiesel and glycerol. Thus, the optimum methanol/oil molar ratio was determined as 6:1.

The biodiesel yield under different catalyst dosage is presented in Fig.6c with methanol/oil molar ratio of 6:1 under 60°C after reacting for 3h. The yield of biodiesel increased from 33.64% to 92.02% with the increment of the catalyst dosage from 0.5wt% to 1.5wt%. While the amount of catalyst was 1.5wt%, the highest yield of biodiesel was reached. Further increase on the catalyst amount will cause the decrease of the yield of biodiesel, because excessive catalyst brings out saponification which will pollute the biodiesel and make it difficult to recover the catalyst. Therefore, the optimum catalyst amount was determined as 1.5wt%.
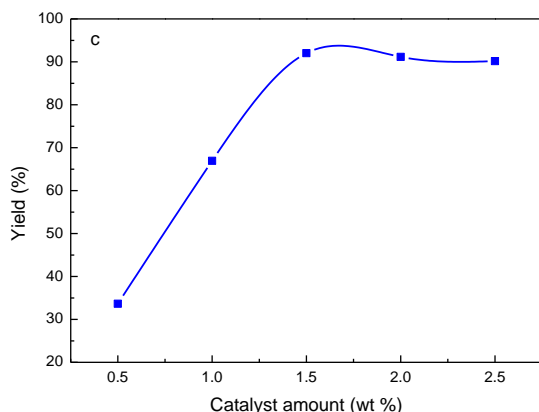
Fig.6. Effect of (c) catalyst amount on yield
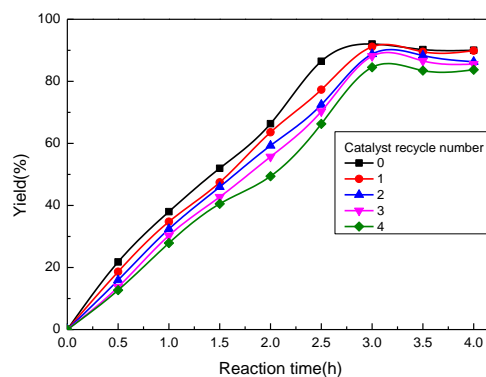
Fig.7. Effect of catalyst cycle number on yield

3.2.2. Reusability of magnetic catalyst

Fig.7 displays the change of biodiesel yield among four times' recycles. It can be seen that the biodiesel yield slightly reduced because of the loss of active components of the catalyst with the number of recycling increased during the processes of reaction and separation. Thus, this magnetic solid base catalyst was proved to maintain considerable catalytic activity after recovery.

4. Conclusions

A magnetic solid base catalyst K/CeO_2-Fe_2O_3 was successfully prepared by sol-gel method and used to convert kitchen lard to biodiesel via transesterification. Kitchen lard was used to simulate stable waste cooking oil to explore the catalytic performance and recyclability of the magnetic solid base catalyst. Based on our experiments, the maximum biodiesel yield of 92.02% was achieved after 3 h under the optimum conditions as follows: reaction temperature of 60°C, methanol/oil molar ratio of 6:1, catalyst amount of 1.5 wt%. After being recycled for four times, the biodiesel yield was maintained more than 84.53% due to its high activity and unique magnetic properties. In summary, K/CeO_2-Fe_2O_3 is a solid base catalyst with high catalytic activity and remarkable recyclability, which make it an ideal substitute for the traditional catalysts.

Acknowledgements

References

[1]   Hassan SZ, Vinjamur M. Chem. Eng. Sci. 2014; 110: 94-104.
[2]   Patil PD, Deng S. Fuel, 2009; 88(7): 1302-1306.
[3]   Meher L C, Sagar D V, Naik S N. Renew. Sust. Energ. Rev., 2006; 10(3): 248-268.
[4]   Kondamudi N, Mohapatra S K, Misra M. Appl. Catal. A-Gen. 2011; 393(1-2): 36-43.
[5]   Verma P, Sharma MP. Renew. Sust. Energ. Rev 2016; 62: 1063-1071.
[6]   Yadav M, Singh V, Sharma YC. Energ Convers. Manage. 2017; 148: 1438-1452.
[7]   Cheng J, Qiu Y, Huang R. Bioresour. Technol. 2016; 221: 344-349.

[8]   Liu K, Wang R. Pet. Coal, 2013, 55(1): 68-72.
[9]   Lee A F, Wilson K. Catal. Today. 2015; 242: 3-18.
[10]   Fattah IMR, Masjuki HH, Kalam MA. Energ Convers. Manage. 2014; 79: 265-272.
[11]   Liu K, Wang R, Yu M. RSC Adv. 2017; 7(82): 51814-51821.
[12]   Liu X, He H, Wang Y. Fuel, 2008; 87(2): 216-221.
[13]   Shu Q, Gao J, Nawaz Z. Appl. Energ., 2010; 87(8): 2589-2596.
[14]   Yu X, Wen Z, Li H. Fuel, 2011; 90(5): 1868-1874.
[15]   Wong YC, Tan YP, Taufiq-Yap YH. Fuel, 2015; 162: 288-293.
[16]   Thitsartarn W, Maneerung T, Kawi S. Energy 2015; 89: 946-956.
[17]   Zhao X, Luo L, Liu C. Chem. Res. &Appl., 2007; 19 (8): 858-862.
[18]   da Conceição L R V, Carneiro L M, Giordani D S, et al. Renew. Energ., 2017; 113: 119-128.
[19]   Al-Abadleh H A, Al-Hosney H A, Grassian V H J. Mol. Catal. A: Chem. 2005; 228(1-2): 47-54.

To whom correspondence should be addressed: prof. Rui Wang, School of Environmental Science and Engineering, Shandong University, No. 27 Shanda South Road, Jinan 250199, China, ree_wong@hotmail.com